International Journal of Chemistry Studies
www.chemistryjournal.in
ISSN: 2581-348X
Received: 21-10-2025, Accepted: 20-11-2025, Published: 04-12-2025
Volume 9, Issue 2, 2025, Page No. 45-52

Green synthesis and characterization of silver nanoparticles using *Ocimum Sanctum* leaf extract and evaluation of their antimicrobial activity

Yogasri G[1], Marx Nirmal R[2*], Sivakumar G M[3], Selvan P[4]

[1] Scholar, Department of Dairy Chemistry, College of Food and Dairy Technology, Koduveli, Tamilnadu Veterinary and Animal Sciences University, Chennai, Tamil Nadu, India

[2] Assistant Professor, Department of Food Process Engineering, College of Food and Dairy Technology, Koduveli, Tamilnadu Veterinary and Animal Sciences University, Chennai, Tamil Nadu, India

[3] Professor, Department of Food Safety and Quality Assurance, College of Food and Dairy Technology, Koduveli, Tamilnadu Veterinary and Animal Sciences University, Chennai, Tamil Nadu, India

[4] Professor, Department of Livestock Products Technology (Meat Science), Madras Veterinary College, Tamilnadu Veterinary and Animal Sciences University, Chennai, Tamil Nadu, India

Abstract

To synthesize eco-friendly silver nanoparticles utilizing *Ocimum sanctum* leaf extract, offering a sustainable alternative to chemical synthesis methods and minimizing the need for microbial routes involving bacteria and fungi. The present study was undertaken to assess the effectiveness of green-synthesized silver nanoparticles (AgNPs). The nanoparticles were prepared using *Tulsi* (*Ocimum sanctum*) leaf extract, which served as both a reducing and stabilizing agent. The biosynthesis was initiated by adding the leaf extract to a 0.01 M silver nitrate solution, resulting in a rapid colour change from yellow to brown, indicating nanoparticle formation, which was confirmed through multiple characterization techniques. UV–Visible spectroscopy revealed a characteristic peak at 413 nm, confirming nanoparticle formation. The particle size was determined as 24.9 nm and zeta potential analysis indicated a charge of −10 mV, reflecting good colloidal stability. EDX analysis confirmed the elemental composition as 70.4% silver, while X-ray diffraction (XRD) established a crystalline size of 14.71 nm with a face-centred cubic structure. Scanning Electron Microscopy (SEM) showed spherical nanoparticles with smooth surfaces. The AgNPs demonstrated strong antimicrobial activity against *Escherichia coli* (16.10 ± 0.09 mm) and *Salmonella typhimurium* (17.20 ± 0.17 mm) at 1 mg/mL concentration. The green-synthesized silver nanoparticles showed excellent stability and significant antimicrobial potential.

Keywords: Silver nanoparticles, *Ocimum Sanctum*, antimicrobial activity, UV–Visible spectroscopy, SEM, EDX, XRD

Introduction

Nanotechnology represents one of the most progressive and multidisciplinary fields in modern science, enabling the creation and manipulation of materials at the nanometer scale. Among the wide variety of nanomaterials, silver nanoparticles (AgNPs) have drawn exceptional scientific interest due to their unique physicochemical and biological characteristics, such as strong antimicrobial properties (Rai *et al.,* 2009) [1]. These properties make AgNPs highly valuable across several sectors, including healthcare, diagnostics, textiles, food technology and environmental management (Burdușel *et al.,* 2018) [2].

Ahmed *et al.* (2016) [3] discussed about the conventional synthesis of silver nanoparticles commonly involves chemical and physical techniques that demand significant energy and employ hazardous reducing agents such as sodium borohydride and hydrazine. While these methods are efficient, they pose serious environmental and biological safety concerns because of the use of toxic chemicals and by-products.

To mitigate these drawbacks, green synthesis has emerged as an environmentally friendly and sustainable alternative. This approach makes use of biological materials - such as plant extracts, bacteria, fungi and algae - as natural reducing and stabilizing agents for nanoparticle formation (Iravani, 2011) [4].

Ocimum sanctum (commonly known as Tulsi or Holy Basil) is an important medicinal herb widely recognized for its therapeutic properties, including antimicrobial, antioxidant and anti-inflammatory activities (Pattanayak *et al.,* 2010) [5]. Its rich phytochemical composition makes it a promising candidate for the biosynthesis of metallic nanoparticles.

Green-synthesized silver nanoparticles are known for their potent antimicrobial action against a variety of pathogenic bacteria. Their mechanism involves direct interaction with microbial cell membranes, disruption of vital metabolic pathways and induction of reactive oxygen species (ROS), leading to structural damage and eventual cell death (Marambio-Jones and Hoek, 2010) [6].

The current research focuses on the green synthesis and characterization of silver nanoparticles using *Ocimum sanctum* leaf extract and the evaluation of their antimicrobial activity against *Escherichia coli* and *Salmonella typhimurium*. This study aims to develop an eco-friendly synthesis method while emphasizing the stability, morphology and biological effectiveness of the biosynthesized nanoparticles.

Materials and Methods

Materials

Chemicals: Silver Nitrate, Gum Arabic, Glycerol Mono Stearate and Citric acid were purchased from Srihari Scientific, Chennai, Tamil Nadu.

Leaves: Fresh leaves of *Ocimum sanctum* (Tulsi leaves) were collected from college of food and dairy technology campus.

Methods

Preparation of leaf extract

20 gm of fresh leaves of tulsi (*Ocimum sanctum*) were collected and washed with normal water followed by distilled water to remove dust particles. Leaves were added to 100 mL of distilled water and boiled at 60 °C for 1 h in sterilized water bath. After boiling, the mixture was cooled and filtered with Whatman paper No. 1. The filtrate was collected and was stored at 4 °C for further analysis. Figure 1 illustrates the process of tulsi leaf extract preparation.

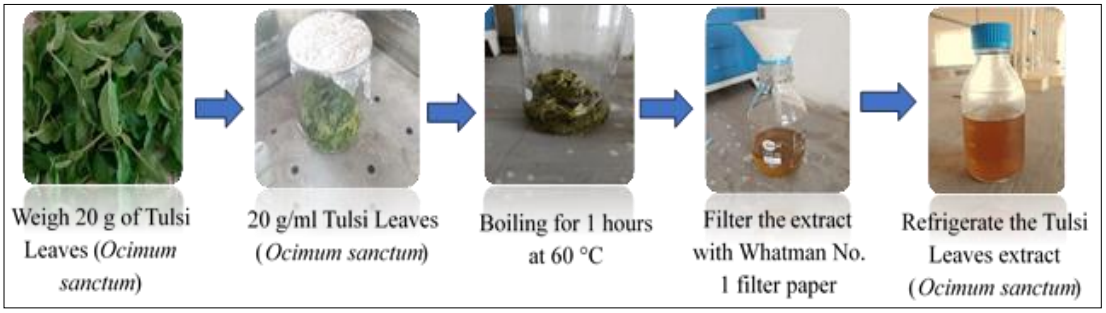

Fig 1: Process of Tulsi leaf (*Ocimum sanctum*) extract preparation

Phytochemical Test (Qualitative) of *Ocimum sanctum* Leaves Extract

Flavonoids test

1 ml of leaf extract was taken in the test tube. 5 ml of dilute ammonia and few dops of concentrated sulphuric acid was added into the test tube. Appearance of yellow colour indicates the presence of flavonoids.

Tannin test

1 ml of leaf extract was taken in the test tube. 1 ml of 0.02M potassium ferrocynaide and 1ml of 0.01M ferric chloride was added into the test tube. Appearance of blue-black colour indicates the presence of tannin.

Quinones test

1 ml of leaf extract was taken in the test tube. 1 ml of sulphuric acid was added into the test tube. Appearance of red colour indicate the presence of quinone.

Glycosides test

1 ml of leaf extract was taken in the test tube. 2 ml of glacial acetic acid, 1 drop of ferric chloride and 1 ml of concentrated sulphuric acid was added into the test tube. Appearance of brown ring indicates the presence of glycoside.

Alkaloids test

1 ml of leaf extract was taken in the test. Few drops of Wagner's reagent were added into the test tubes. The reddish-brown precipitate indicates the presence of alkaloids.

Steroids test

2 ml of the leaf extract was taken in a test tube. Then, 2 ml of chloroform and a few drops of sulfuric acid and acetic acid were added. The development of a greenish colour indicated the presence of steroids.

Terpenoids test

1 ml of leaf extract was taken in the test tube. 2 ml of chloroform and 3 ml of concentrated H_2SO_4 was taken into the test tube. Appearance of reddish-brown colour indicate the presence of terpenoids.

Saponin test

2 ml of distilled water and 2 ml of leaf extract taken in the test tube. After shaking, foam formation indicates the presence of saponin.

Synthesis of silver nanoparticle

For synthesis of silver nanoparticle, Tulsi leaves extract was added to 0.01M silver nitrate solution at different concentration.

The silver ions were reduced to silver nanoparticle within few minutes by Tulsi leave extract. The conversion of solution colour showed the formation of silver nanoparticle by observing colour change from yellow colour to brown colour. Then calcinated to get nanoparticle powder. Figure 2 illustrate the process of green synthesis of Silver Nanoparticle.

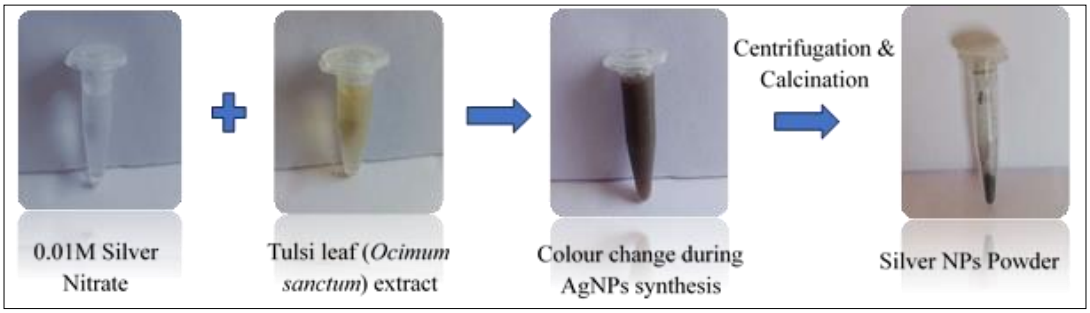

Fig 2: Process of green synthesis of Silver Nanoparticle

Characterisation of synthesised silver nanoparticle

UV-Visible spectroscopy of AgNPs

UV-visible spectra of AgNPs were determined at a wavelength range of 200-800 nm with Epoch microplate spectrophotometer, US.

Particle size and Zeta potential of AgNPs

Hydrodynamic size distribution and zeta potential of the synthesized AgNPs was measured using Horibia Zeta Sizer instrument, Kyoto, Japan. Zeta potential estimated the stability of nanoparticles by measuring the surface charge of the nanoparticles.

Antimicrobial activity of AgNPs

Antimicrobial activity of AgNPs was tested using agar well diffusion method against gram negative microorganisms *viz*. *E. coli* and *Salmonella typhimuriyum*. The optical density of bacterial cultures was maintained at the standard 0.5 for MacFarland by addition of sterilized Mueller-Hinton broth. Each bacterial culture was uniformly spread on solidified sterile Mueller-Hinton Agar plates using sterile cotton swabs and left for 10 minutes for absorption. The agar plates were punched for making wells of 6 mm diameter using a sterilized cork borer. The wells were filled with 50 µL of four different concentrations of synthesized AgNPs (1mg/mL, 500µg/mL, 250µg/mL and 125µg/mL). Kanamycin monosulphate (1mg/ml) was used as a standard antibiotic drug. The plates were then incubated for 24 h at 37° C and the diameter of clearing zone of inhibition was measured in millimetres using the ruler scale (Amrulloh *et al.,* 2021)

Scanning electron microscopy of AgNPs

Scanning electron microscopy was used for studying the morphological structures of the synthesized AgNPs. The analysis was performed using Esprit 1.9, Bruker Nano GmbH Berlin, Germany scanning electron microscope with XFlash 5010 detector.

Elemental composition of AgNPs

The elemental composition and particle distribution of the synthesized AgNPs was studied using Energy Dispersive X-Ray (EDX) analysis performed in Esprit 1.0, Bruker Nano GmbH Berlin, Germany scanning electron microscope with XFlash 5010 detector. AgNPs was spread on the top of the sample holder for gold sputtering to perform EDX analysis.

X-ray diffraction analysis of AgNPs

An X-ray diffractometer (PANalytical, Netherlands) was used to analyze the crystal structure of the developed AgNPs. All measurements were conducted using a scan range of 10°-90° and a step size 2 θ = 0.022. In addition, XRD peak broadening analysis was carried out to evaluate the average crystallite size of the synthesized nanoparticles through the Debye Scherrer formula.

$$D = \frac{\kappa\lambda}{\beta cos\theta}$$

Where,

D = particle size of the crystal

κ = Scherrer constant (usually 0.9),

λ = wavelength of X-ray source, CuKα radiation (0.154059 nm (or) 1.54059Å),

β = full width at half-maximum (FWHM) of the diffraction peak in radian

θ = Bragg's diffraction angle.

Result and Discussion

Phytochemical analysis (Qualitative) of *Ocimum sanctum* Leaves Extract

The result of qualitative phytochemical test of tulsi leaf extract was given in the table 1. Figure 3 shown the phytochemical analysis of tulsi leaf extract. The phytochemical analysis of the leaf extract revealed the presence of various secondary metabolites including flavonoids, tannins, quinones, glycosides, alkaloids, steroids, terpenoids and saponins. The phytochemicals act as reducing agent in the synthesis of silver nanoparticles. During green synthesis, phytochemicals serve as natural reducers, converting Ag^{+} ions into silver nanoparticles.

The results were found to be consistent with the findings of Naik *et al.* (2015) [7], who conducted a phytochemical analysis of *Ocimum tenuiflorum* leaf extract.

Table 1: Phytochemical analysis (Qualitative test) of *Ocimum sanctum* Leaves Extract

S.NO	Phytochemicals	Qualitative test
1	Flavonoids	+
2	Tannin	+
3	Quinones	+
4	Glycosides	+
5	Alkaloids	+
6	Steroids	+
7	Terpenoids	+
8	Saponin	+

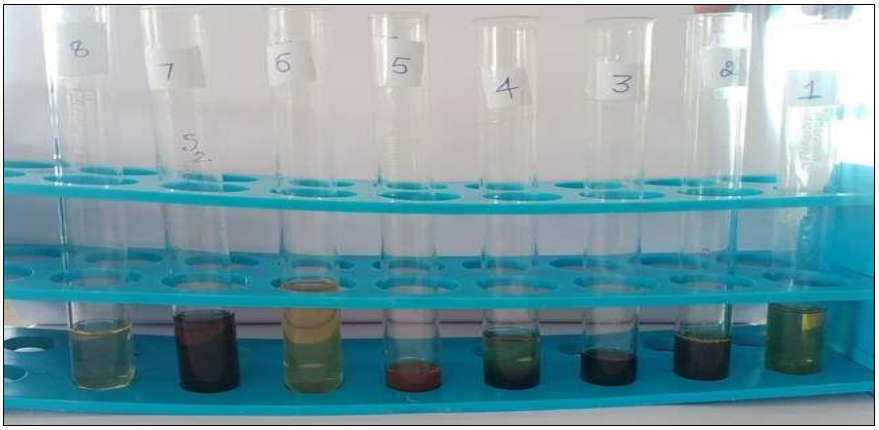

Fig 3: Phytochemical analysis of tulsi leaf extract

Characterization of AgNPs

UV-Visible spectroscopy of AgNPs

The UV- Visible characterisation was carried out for the qualitative confirmation of silver nanoparticle (AgNPs) synthesis based on their characteristic absorption spectra of AgNPs.

The characteristic absorption peak of the synthesized AgNPs was observed at 420 nm, which falls within the range of 400-420 nm as reported by Prathibha *et al.* (2024) [10]. They synthesized AgNPs using *Ocimum tenuiflorum* and *Azadirachta indica* extracts and recorded absorption peaks at 420 nm and 408 nm, respectively.

UV-visible spectroscopy was performed to qualitatively confirm the formation of nanoparticles through their characteristic absorption. The synthesized AgNPs exhibited a characteristic peak at 420 nm, confirm the successful formation of silver nanoparticle.

Similarly, Sulaiman *et al.* (2024) [8] reported a characteristic peak at 420 nm for AgNPs synthesized from *Ocimum sanctum* extract. Similarly, Saxena *et al.* (2010) [9] reported characteristics peak at 412.94 nm for AgNPs synthesized from extract onion (*Allium cepa*).

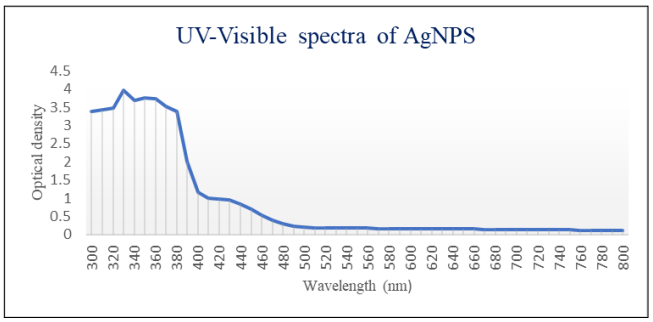

Fig 4: UV-Visible spectra of AgNPs

Particle size and zeta potential of AgNPs

Dynamic light scattering (DLS) was used to analyse the hydrodynamic size distribution of AgNPs in a colloidal solution. The size distribution was found as 123 nm. Figure 5 (a) given the Particle Size of AgNPs. Similar result was obtained by Siakavella *et al.* (2020) [11] with size distribution of 137.5 ± 0.76 nm for AgNPs synthesized from sea buckthorn.

Similar result was obtained by Mat Yusuf *et al.* (2020) [12] with size distribution of 114.7 ± 1.012 nm for AgNP-Leaf and 129.9±1.400 nm for AgNP-Stem synthesized from *Clinacanthus nutans*. Similarly, the result obtained by Somda *et al.* (2024) [13] with size distribution of 196.4 ± 2.12 nm for AgNPs synthesized from *Brassica carinata*. The size obtained through DLS is a combination of the particles and hydrodynamic radius, which includes both the nanoparticles and the surrounding hydration layer; therefore, it does not represent the actual core size of the silver nanoparticle (Gavamukulya *et al.,* 2020) [15]. Thus, the DLS analysis confirmed that the synthesized AgNPs exhibited a hydrodynamic radius of 123 nm, indicating stable nanoparticle dispersion in the colloidal solution.

Zeta potential values between 0 and ±10 are considered as highly unstable in colloidal solution and tend to settle. Zeta potential values between ±10 mV and 20 mV are considered as stable and values above +30 are found to be highly stable. The zeta potential of the synthesized AgNPs was found as -10.0 mV and this value indicates the stability of AgNPs in colloidal solutions.

Thus, the zeta potential value of -10 mV suggests that the synthesized AgNPs exhibit moderate stability in colloidal solution, preventing rapid aggregation but not representing highly stable nanoparticles.

The negative sign indicates that the stability is due to the repulsive force between the particles. Similar result was observed by Siakavella *et al.* (2020) [11] with a zeta potential of -29.77 ± 0.40 mV.

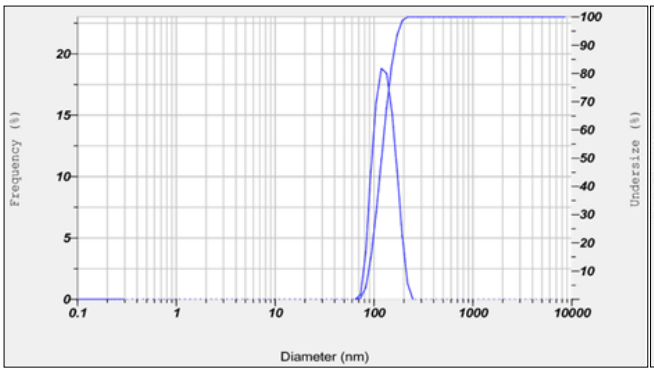

Fig 5: (a) Particle Size of AgNPs

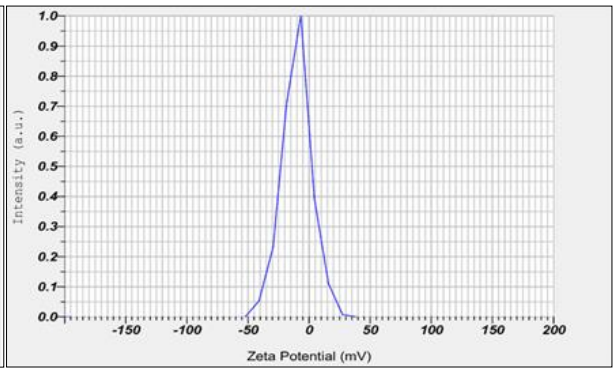

Fig 5: (b) Zeta potential of AgNPs

Antimicrobial activity of AgNPs

Table 2 shows the results of antimicrobial activity of AgNPs against *E. coli* and *Salmonella typhimurium*. Figure 6 (a) shows the inhibition zones developed by AgNPs against *E. coli*. Figure 6 (b) shows the inhibition zones developed by AgNPs against *Salmonella typhimurium*.

The antimicrobial activity of the AgNPs was observed highest at 1 mg/ml concentration for both *E. coli* and *Salmonella typhimurium* with inhibition zones measuring 16.10 ± 0.096 mm and 17.20 ± 0.171 mm respectively. The lowest inhibition zones were observed at 125 µg/ml with 6.30 ± 0.203 mm and 7.20 ± 0.096 mm for both *E. coli* and *Salmonella typhimurium* respectively. The standard (Kanamycin) showed larger inhibition zones measuring 25.20 ± 0.129 mm for both *E. coli* and *Salmonella typhimurium*.

Statistical analysis showed a highly significant (P≤0.01) different between the concentration of the AgNPs on the antimicrobial activity.

Previous studies have demonstrated similar antimicrobial activities of AgNPs 16.23 ± 0.68 against *E. coli* Somda *et al.* (2024) [13]. Feroze *et al.* (2020) [14] identified that, at 5mM dilution of 40µl, AgNPs showed 18.3 ± 0.60 mm zone of inhibition against *Salmonella typhimurium*

Table 2: Antimicrobial activity of AgNPs against *E. coli* and *Salmonella typhimurium*

S. no	Concentration (µg/ml)	Zone of Diameter (mm)		T value
		(*Escherichia Coli*)	(*Salmonella typhimurium*)	
A	1 mg/ml	16.10 ± 0.096^{d}	17.20 ± 0.171^{d}	5.594^{**}
B	500 µg/ml	15.25 ± 0.187^{c}	12.25 ± 0.183^{c}	11.421^{**}
C	250 µg/ml	9.50 ± 0.096^{b}	9.20 ± 0.054^{b}	0.539^{NS}
D	125 µg/ml	6.30 ± 0.203^{a}	7.20 ± 0.096^{a}	3.998^{**}
E	Standard	25.20 ± 0.129^{e}	25.20 ± 0.129^{e}	0^{NS}
F value		2345.544^{**}	666.317^{**}	

Fig 6 a: Antimicrobial Activity of AgNPs against *E.coil*

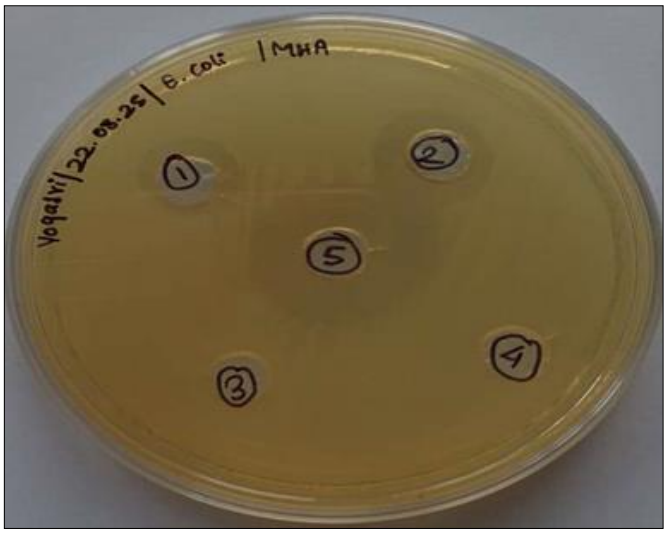

Fig 6 b: Antimicrobial Activity of AgNPs against *Salmonella typhimurium*

Scanning electron microscopy of AgNPs

Figure 7 (a), Figure 7 (b) and Figure 7 (c) show the scanning electron microscopic image of AgNPs at 1µm, 400nm and 200 nm level respectively. It is found that AgNPs are spherical in nature, clustered together and exhibit smooth surface. The average size of the synthesized AgNPS is 24.9 nm. Somda *et al.* (2024) [13] synthesized AgNPs using *Brassica carinata* microgreens and scanning electron microscopy (SEM) revealed that the nanoparticles were spherical with a smooth and even surface texture.

Likewise, Sulaiman *et al.* (2024) [8] also synthesized a AgNPs using *Ocimum Sanctum* extract, where scanning electron microscopy analysis revealed that the particles are spherical, with an average size of 23.82 ± 4.17 nm. Mohammed and Hawar (2022) [16] green synthesized AgNPs using *Moringa oleifera* leaves and scanning electron microscopy imaging confirmed spherical shaped nanoparticles with an average size of 17 nm.

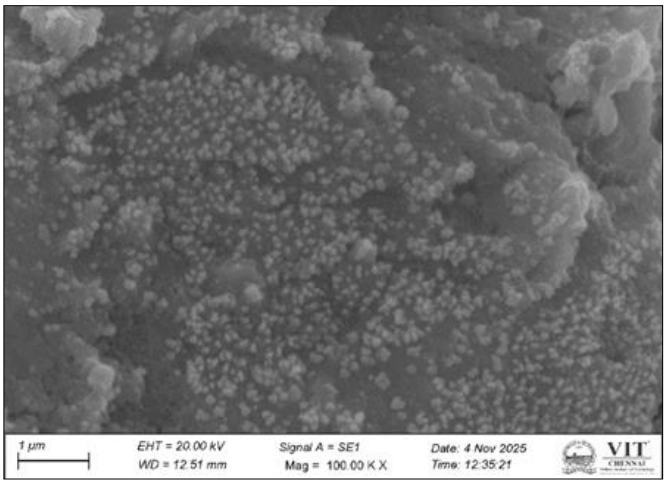

Fig 7 a: Scanning electron microscopic image of AgNPs at 1µm

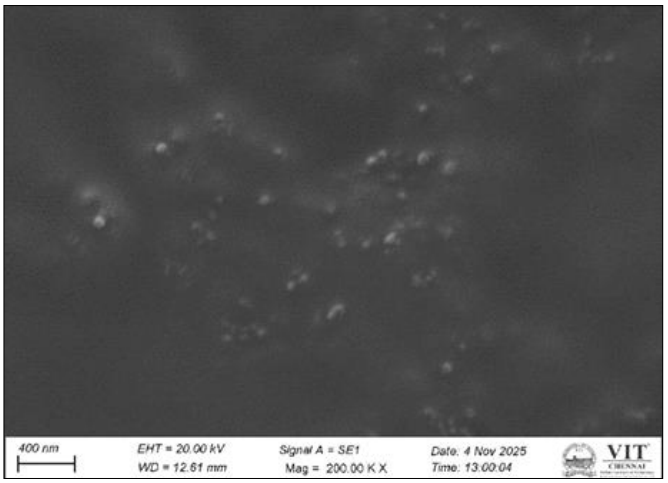

Fig 7 b: Scanning electron microscopic image of AgNPs at 400nm

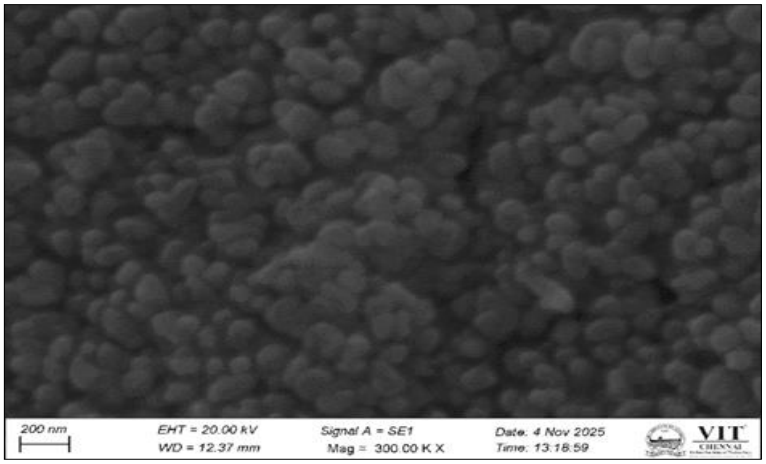

Fig 7 c: Scanning electron microscopic image of AgNPs at 200nm

Elemental composition of AgNPs

The elemental composition of the synthesized silver nanoparticles (AgNPs) revealed that they were predominantly composed of silver (Ag), which accounted for 70.40 per cent of the total weight. Other elements detected included carbon (12.80 per cent), chlorine (10.30 per cent) and oxygen (6.40 per cent). The high proportion of silver confirms the successful formation of AgNPs. Table 3 shows the elemental composition of AgNPs, while the distribution of silver molecules within the nanoparticles is represented in Figure 8. Therefore, the EDX analysis confirmed the successful formation of AgNPs, with silver being the major constituent, while the presence of carbon, chlorine and oxygen likely originated from plant phytochemicals and residual stabilizing agents associated with the green synthesis process. A fairly similar results were observed by Somda *et al.* (2024) [13] with 71.2 per cent silver, 13.7 per cent chlorine, 12.6 per cent carbon, 1.8 per cent oxygen and 0.7 per cent sulphur.

Table 3: Elemental Composition of AgNPs

Element	Weight (Per cent)	Atomic (Per cent)	Net Intensity
C K	12.8	44.3	48.0
O K	6.4	16.7	36.0
Cl K	10.3	12.1	622.4
Ag L	70.4	27.0	1443.4

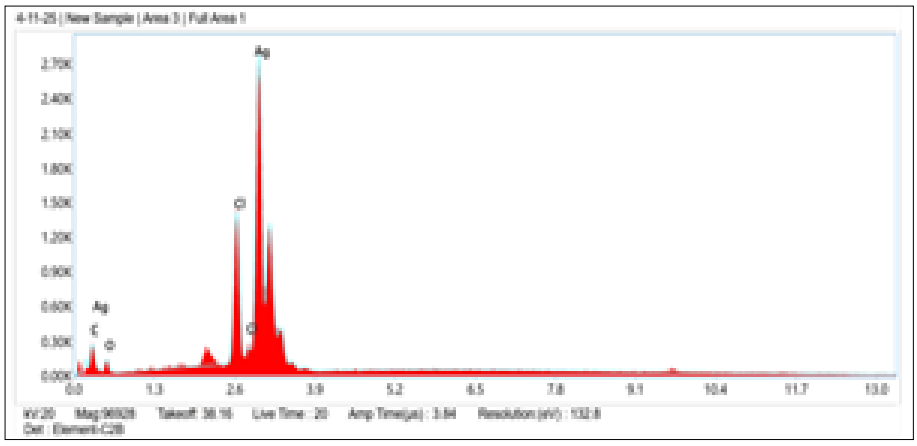

Fig 8: EDX analysis of AgNPs

X-ray Diffraction analysis of AgNPs

The X-ray diffraction spectra of AgNPs is illustrated in Figure 9 and XRD result of AgNPs are illustrated in Table 4. The average diameter of the nanoparticle based on the Debye – Scherrer equation was 14.71 nm. The results pertaining to X-ray diffraction analysis of AgNPs identified various forms of AgNPs at different 2 theta angles – where 38.02, 44.24, 64.49 and 77.29 corresponds to cubic Ag (Mehta *et al.,* 2017) [17] and corresponding to the reflection planes of (111), (200), (220) and (311) respectively, indicates the face-centred spherical structure of silver. The compound prediction is based on JCPDS file no. 04-0783.

The average crystallite size of synthesized AgNPs based on the Debye - Scherrer equation was 14.71 nm. The synthesised AgNPs with an average crystallite size of 22.88 nm (Somda *et al.,* 2024) [13].

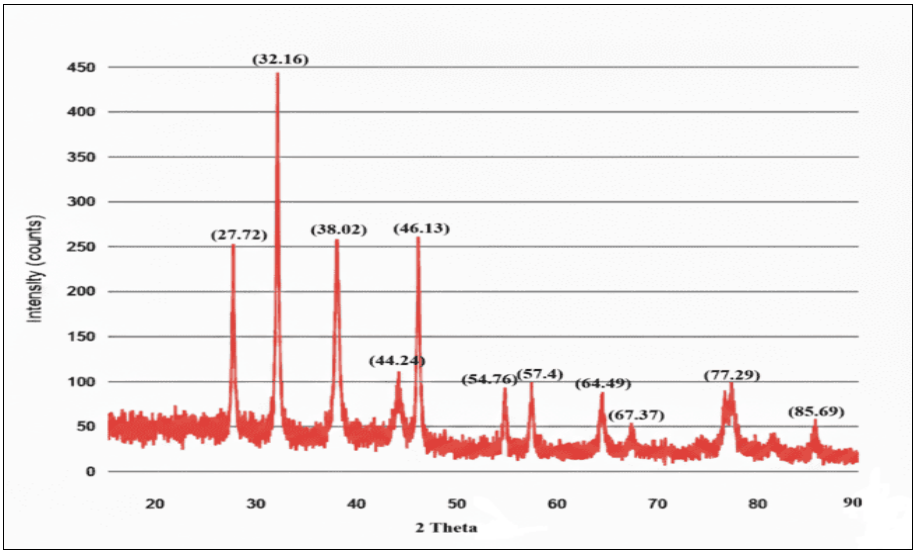

Fig 9: X-ray diffraction spectra of AgNPs

Table 4: X-ray diffraction result of AgNPs

2θ	Cos θ	Sin θ	FWHM (degree)	β (radian)	Crystalline size 'D' nm	Inter planar spacing 'd' Å	h k l identified from peak	$h^2+k^2+l^2$ from identified h k l	Lattice constant 'a' from d Å	Cell volume $Å^3$
38.02	0.945	0.326	0.460	0.00803	18.27	2.3628	1 1 1	3	4.0923	68.53
44.24	0.927	0.377	0.70	0.0122	12.26	2.0432	2 0 0	4	4.0864	68.23
64.49	0.847	0.534	0.540	0.00942	17.37	1.4425	2 2 0	8	4.0793	67.88
77.29	0.782	0.625	0.930	0.0162	10.94	1.2324	3 1 1	11	4.0866	68.24

Discussion

The silver nanoparticles were synthesized using the green synthesis method with tulsi (*Ocimum sanctum*) leaf extract acting as a natural reducing and stabilizing medium. The synthesis of silver nanoparticles was indicated by a visible colour transition from yellow to brown and subsequently verified through multiple analytical characterization techniques. UV - visible spectral analysis revealed a characteristic peak at 420 nm, indicating the successful synthesis of silver nanoparticles (AgNPs). The synthesized nanoparticles had a particle size of 123 nm and a zeta potential value of –10 mV, indicating good stability were analysed by particle size analyser. Scanning Electron Microscopy (SEM) found that AgNPs are spherical in nature, clustered together and exhibit a smooth surface with an average size of 24.9 nm and Energy Dispersive X-ray (EDX) analysis confirmed that silver accounted for 70.4% of the total weight. The X-ray diffraction (XRD) analysis confirmed the crystalline nature of AgNPs with reflection planes corresponding to Face-centred cubic structure. The antimicrobial activity of the synthesized nanoparticles showed strong inhibitory zones against *Escherichia coli* and *Salmonella typhimurium*, proving their effectiveness as antimicrobial agents.

Acknowledgement

Part of the research work was submitted to College of Food and Dairy Technology, Koduveli, Tamil Nadu Veterinary and Animal Sciences University, Chennai - 52 by the M. Tech Scholar in partial fulfilment for the award of M. Tech degree.

Reference

1. Rai M, Yadav A, Gade A. Silver nanoparticles as a new generation of antimicrobials. Biotechnology Advances,2009:27(1):76–83.
2. Burdușel AC, Gherasim O, Grumezescu AM, Mogoantă L, Ficai A, Andronescu E, *et al*. Biomedical applications of silver nanoparticles an up-to-date overview. Nanomaterials,2018:8(9):681.
3. Ahmed S, Ahmad M, Swami BL, Ikram S. A review on plants extract mediated synthesis of silver nanoparticles for antimicrobial applications a green expertise. Journal of Advanced Research,2016:7(1):17–28.
4. Iravani S. Green synthesis of metal nanoparticles using plants. Green Chemistry,2011:13(10):2638–2650.
5. Pattanayak P, Behera P, Das D, Panda SK. *Ocimum sanctum* Linn. A reservoir plant for therapeutic applications an overview. Pharmacognosy Reviews,2010:4(7):95.
6. Marambio-Jones C, Hoek EM. A review of the antibacterial effects of silver nanomaterials and potential implications for human health and the environment. Journal of Nanoparticle Research,2010:12(5):1531–1551.
7. Naik LS, Shyam P, Marx KP, Baskari S, Devi VR. Antimicrobial activity and phytochemical analysis of Ocimum tenuiflorum leaf extract. International Journal of PharmTech Research,2015:8(1):88–95.
8. Sulaiman M, Muhammad MAA, Sulaiman AS, Abubakar AL, Sharma R, Shuaibu AM, *et al*. Antimicrobial potential and characterization of silver nanoparticles synthesized from *Ocimum sanctum* extract. bioRxiv,2024:2024–09.
9. Saxena A, Tripathi RM, Singh RP. Biological synthesis of silver nanoparticles by using onion (Allium cepa) extract and their antibacterial activity. Digest Journal of Nanomaterials and Biostructures,2010:5(2):427–432.
10. Prathibha BS, Harshitha N, Neha DR, Pranathi CN, Kumar DV, Lakshmi GC. Green synthesis of silver nanoparticles using Ocimum tenuiflorum and

Azadirachta indica leaf extract and their antibacterial activity. Journal of Physics Conference Series,2024:2748(1):012015.
11. Siakavella IK, Lamari F, Papoulis D, Orkoula M, Gkolfi P, Lykouras M, Hatziantoniou S. Effect of plant extracts on the characteristics of silver nanoparticles for topical application. Pharmaceutics,2020:12(12):1244.
12. Mat Yusuf SNA, Che Mood CNA, Ahmad NH, Sandai D, Lee CK, Lim V. Optimization of biogenic synthesis of silver nanoparticles from flavonoid-rich Clinacanthus nutans leaf and stem aqueous extracts. Royal Society Open Science,2020:7(7):200065.
13. Somda D, Bargul JL, Wesonga JM, Wachira SW. Green synthesis of Brassica carinata microgreen silver nanoparticles characterization safety assessment and antimicrobial activities. Scientific Reports,2024:14(1):2 9273.
14. Feroze N, Arshad B, Younas M, Afridi MI, Saqib S, Ayaz A, *et al*. Fungal mediated synthesis of silver nanoparticles and evaluation of antibacterial activity. Microscopy Research and Technique,2020:83(1):72–80.
15. Gavamukulya Y, Maina EN, Meroka AM, Madivoli ES, El-Shemy HA, Wamunyokoli F, *et al*. Green synthesis and characterization of highly stable silver nanoparticles from ethanolic extracts of fruits of Annona muricata. Journal of Inorganic and Organometallic Polymers and Materials,2020:30(4):1231–1242.
16. Mohammed GM, Hawar SN. Green biosynthesis of silver nanoparticles from Moringa oleifera leaves and its antimicrobial and cytotoxicity activities. International Journal of Biomaterials,2022:2022(1):4136641.
17. Mehta BK, Chhajlani M, Shrivastava BD. Green synthesis of silver nanoparticles and their characterization by XRD. Journal of Physics Conference Series,2017:836(1):012050.